PAPER ID ICLASS06-185

Direct Numerical Simulation of Non-Newtonian Droplet Deformation

Bowen P.J., Phillips T.N. and Zheng Y.
Cardiff University BowenPJ@cf.ac.uk, PhillipsTN@cardiff.ac.uk

Abstract

Spectral element methods are developed for solving two-phase flow problems of relevance to two-phase power generation systems (e.g. IC and gas turbines engines), environmental protection (e.g. halon-free explosion suppression) and a range of non-Newtonian fluids. In particular, a direct numerical simulation is presented for the benchmark problem of a Newtonian droplet deforming and accelerating from rest in a uniform gas field, and here this DNS model is extended to include a range of inelastic non-Newtonian fluids. The governing equations for incompressible fluids are conveniently written in terms of four dimensionless groups for ease of parametric numerical experiments : Reynolds number, Weber number and the viscosity and density ratios of the two fluids. The four-parameter Cross viscosity model is introduced to extend the analysis to non-Newtonian fluids. The arbitrary Lagrangian-Eulerian (ALE) formulation is used to account for the movement of the mesh. Spectral element approximations are used to ensure high degree of spatial accuracy. The computational domain is decomposed into two regions, one of which remains fixed in time while the other, located in the vicinity of the droplet, is allowed to deform within the ALE framework. Transfinite mapping techniques are used to map the physical elements onto the computational element, surface tension is treated implicitly and naturally within the weak formulation and the viscosity model is introduced explicitly within the numerical formulation. Whereas the advantages and accuracy of the Spectral-element method is discussed in detail elsewhere, here sample results demonstrate the potential of the methodology for free boundary deformation problems by considering the influence of Weber number, Reynolds number, viscosity ratio and an exemplar non-Newtonian model for blood on the deformation of the free droplet boundary. Boundary oscillations of the extremities of the deformed droplet about its centre are predicted, which stabilise in the upstream and downstream direction for high and low Weber number respectively. It is suggested that this may be an indicator of the onset of breakup. Higher Reynolds number appears to dampen oscillatory behaviour, whilst high viscosity ratio inhibits deformation, and the non-Newtonian blood model shows unusual deformation topologies.

Keywords: Droplet deformation, spectral-element, arbitrary Lagrangian-Eulerian method, non-Newtonian, blood

1 INTRODUCTION

Deformation of fluid elements (e.g. droplets) in a flowstream of a secondary fluid, is a precursor to fluid breakup, a fundamental process in atomisation. These problems occur in a diverse range of applications both in industry and nature, from the efficient utilisation of liquid fuel in IC and gas turbine engines, to the effective utilisation of water sprays as Halon-replacement suppressants of accidental explosions, to the deformation of raindrops or the atomisation of blood particles in criminology cases. Figure 1 shows a high-speed image of a droplet deforming prior to break-up in an air-stream. Empirical analyses of the droplet breakup process may be found elsewhere (1, 2), with most referring to the 'critical Weber number' approach.

Whilst numerical simulation codes have now been developed to a stage whereby meaningful predictions may be generated for industrial two-phase problems (3), there are still considerable limitations due to the computational requirements of more common numerical techniques such as finite volume methodologies. This provides the motivation to develop ever more efficient numerical methods to address complex, computationally expensive problems such as those considered in this paper.

Figure 1. High-speed Image of Droplet Deformation Prior to Breakup in an Air-Flow (left-to-right)

The principle challenge in the numerical simulation of the interactions between two immiscible fluids is the ability to track the interface between a fluid, which is arbitrarily-shaped and translating. There are two standard approaches that can be employed for tracking the location of the free surface between the two fluids, viz. the Eulerian and Lagrangian approaches. However, the shortcomings of both approaches prompted the development of what are known

as arbitrary Lagrangian-Eulerian techniques (4, 5, 6, 7). The methods utilise the advantages of both the Lagrangian and Eulerian formulations, whilst at the same time avoiding their drawbacks. The ALE approach may be considered as a computational reference system that can be chosen quite arbitrarily and which is continually changing in order to allow for the precise description of moving interfaces, ensuring the integrity of the mesh over time.

In previous numerical simulations (8) a body force is applied to the droplet to prevent it from accelerating until it reaches its free-stream velocity. This constraint is not imposed in other work (9) nor the present study, so that as in practical problems, the droplet is free to translate downstream whilst deforming.

Here, sample results for both the Newtonian and non-Newtonian droplet deformation problem are presented. In sections 2 and 3, the Newtonian and non-Newtonian governing equations are presented. Section 4 summarises the numerical schemes developed, including the final algorithm employed for both fluids. Sample results are presented and discussed in Section 5, before drawing conclusions in Section 6.

2 GOVERNING NEWTONIAN EQUATIONS

It may be shown that the dimensionless equations of mass and momentum for the two Newtonian fluids may be written

$$\nabla \cdot u_g = 0,\ \nabla \cdot u_d = 0 \qquad (1)$$

$$\mathrm{Re}\left(\frac{\partial u_g}{\partial t} + u_g \cdot \nabla u_g\right) = -\nabla p_g + \nabla \cdot T_g \qquad (2)$$

$$\bar{\rho}\,\mathrm{Re}\left(\frac{\partial u_d}{\partial t} + u_d \cdot \nabla u_d\right) = -\nabla p_d + \nabla \cdot T_d \qquad (3)$$

where the extra-stress tensor for each fluid is given by

$$T_g = 2d_g,\ T_d = 2\bar{\eta} d_d \qquad (4)$$

and the dimensionless form of the force balance across the interface becomes :

$$\left(\sigma_d - \sigma_g\right)\cdot n = \left(\frac{\mathrm{Re}}{We}\right)\kappa n \qquad (5)$$

σ_i is the Cauchy-stress tensor for fluid i, and κ is the local radius of curvature of the interface which can be written

$$\kappa = \left(\frac{1}{R_1} + \frac{1}{R_2}\right) \qquad (6)$$

The surface tension force at an interface between two fluids depends on the curvature of the interface. In general, for an arbitrarily shaped surface the principle radii of curvature can be determined relatively easily. Let the interface be described parametrically by the curve x = x(s), y = y(s), where s is measured along the interface. Then the radii of curvature for the axi-symmetric surface are given by:

$$\frac{1}{R_1} = \frac{x'y'' - y'x''}{\left[(x')^2 + (y')^2\right]^{3/2}},\ \frac{1}{R_2} = \frac{x'}{y\left[(x')^2 + (y')^2\right]^{1/2}} \qquad (7)$$

where the primes denote differentiation with respect to s.

Hence, the problem is posed in terms of 4 dimensionless numbers of practical relevance, facilitating independent parametric studies of each grouping, which of course is very difficult to achieve experimentally. These are the familiar (gaseous-based) Reynolds number, (gaseous based) Weber number, density ratio and viscosity ratio of the two fluids.

3 NON-NEWTONIAN MODEL

The extension of the droplet/flow model to include non-Newtonian effects is particularly of interest given the range of practical problems involving fluids which exhibit non-Newtonian characteristics, the potential influence of non-Newtonian parameters in droplet deformation and the fact that hitherto they have been given very limited consideration for this problem. However, the inclusion of non-Newtonian effects in numerical modelling is known generally to increase the difficulty of obtaining converged numerical solutions for complex flow, and so a gradual increase in model complexity has been adopted. Hence, this first development from the Newtonian model considers a fluid model without elasticity, namely a shear-rate dependent viscosity model.

Whilst the simplest non-Newtonian viscosity models comprise two-parameter (e.g. power law) or three-parameter (e.g. Herschel-Buckley, Sisko) models, here the 4-parameter Cross viscosity model (10) is utilised in the interest of generality. The common two and three parameter models referenced are in fact special cases of the Cross model. The Cross model has been utilised previously to describe a broad range of non-Newtonian fluids, including polymer solutions and melts, particulate dispersions, yoghurt, soy protein suspensions, hair shampoo, blood, etc..

The Cross viscosity model as a function of shear-rate has been utilised in the following mathematical form:

$$\eta = \eta_\infty + \frac{\eta_0 - \eta_\infty}{1 + (K\dot{\gamma})^m} \qquad (6)$$

where the four parameters comprise η_0 - the zero shear-rate viscosity, η_∞, - the high shear-rate viscosity asymptote, K and m, where K has dimensions of time, and m is dimensionless.

4 NUMERICAL METHODS

As discussed earlier, a more sophisticated approach to evaluating the partial time derivative within a moving grid system is the arbitrary Lagrangian-Eulerian (ALE) approach. In the ALE formulation, the computational mesh evolves in time and can be chosen quite arbitrarily. Given a

reference frame with velocity **w**, then the partial time derivative can be evaluated by :

$$\frac{\partial}{\partial t} = \frac{\delta}{\delta t} - (w \cdot \nabla) \qquad (7)$$

where δ/δt is the time derivative with respect to the moving reference frame. In this model, the reference frame is taken to be the spectral element grid determined at each time-step.

The Navier-Stokes equations, written in component form, are utilised to derive the weak formulation of the problem (11).

Care must be exercised in defining suitable test functions in the ALE formulation for the sake of consistency, since the function spaces are defined on the time-dependent domain Ω(t), and the time derivative will involve the spatial frame of reference. The test functions **v** must be independent of time in the reference system.

It may be shown (11) that the weak formulation can be written in the form:

$$\frac{\delta}{\delta t}\left(Bu_i\right) = D_i^T p - A_{i,j} u_i + F_i + C_i \qquad (8)$$

$$-D_i u_i = 0 \qquad (9)$$

where A is the discrete diffusion matrix, B is the velocity mass matrix, D_i is the discrete gradient matrix, F_i contains the surface tension contributions and C_i contains the convection terms.

The nodal co-ordinates are updated using

$$\frac{\delta X_i}{\delta t} = w_i \qquad (10)$$

Temporal discretisation is performed using a second-order scheme. The linear terms are discretised implicitly using a second-order backward differentiation scheme and the nonlinear terms are discretised explicitly using a second-order Adams-Bashforth method.

The mesh is moved using :

$$\frac{1}{\Delta t}\left(X_i^{n+1} - X_i^{n}\right) = \frac{3}{2} w_i^n - \frac{1}{2} w_i^{n-1} \qquad (11)$$

In order to set up the corresponding discrete variational formulation of the Stokes problem, it is necessary to choose conforming discrete subspaces of the velocity and pressure spaces. In this paper the problem is discretised using the spectral element method. The domain Ω is partitioned into K non-overlapping quadrilateral spectral elements Ω_k, k = 1,…, K.

Each spectral element is mapped onto the parent element

$$D = \{(\xi, \eta) : -1 \le \xi, \eta \le 1\} \qquad (12)$$

using a transfinite mapping. For elements adjacent to the interface, a hybrid isoparametric transfinite mapping is used.

Using appropriate basis functions (11) the velocity and pressure may be represented in spectral form as

$$u_N(x) = \sum_{j=1}^{Nv} u_j \phi_j(x), \; p_N(x) = \sum_{k=1}^{NQ} p_k \psi_k(x) \qquad (13)$$

and the linear system associated with the discrete form of the system may be shown to be

$$A_N \mathbf{u}_N + B^t_N \mathbf{p}_N = \mathbf{f}_N \qquad (14)$$

$$B_N \mathbf{u}_N - \mu C_N \mathbf{p}_N = 0 \qquad (15)$$

where entries of the matrices A_N, B_N and C_N are specified elsewhere (11).

It follows that the following equation determines $\mathbf{p}_N$

$$(B_N A_N^{-1} B^t_N + \mu C_N)\, \mathbf{p}_N = B_N A_N^{-1} \mathbf{f}_N \qquad (16)$$

It can be shown that the preconditioned conjugate gradient (PCG) method may be used to solve the system, and was used to generate the results presented in this paper.

Finally, the numerical algorithm utilised for this problems takes the form :

(1) Form an initial mesh around and within the droplet. Part of the skeleton spectral element mesh (Ω_f) is fixed, while the remaining portion (Ω_m) is allowed to change in time.
(2) Start with an initial solution at time t = 0 e.g. gas and droplet at rest or the velocity field determined by solving an associated problem for a solid sphere at the same Reynolds number.
(3) Move from time t^n to t^{n+1} by performing the following steps :
    (a) Solve for the mesh movement by solving

$$\frac{\delta X_i^{n+1}}{\delta t} = w_i^{n+1} \qquad (17)$$

    to determine the position of the new vertices on the skeleton spectral element mesh corresponding to Ω_m.
    (b) In non-Newtonian case, evaluate the viscosity function by first evaluating the rate-of-strain at time t^n and then employing within the Cross model
    (c) Update the matrices $A_{i,j}^{n+1}$, B^{n+1}, etc..
    (d) Solve for the velocity and pressure at the new time level using the preconditioned conjugate gradient method.
    (e) Obtain the new mesh velocity and repeat.

5 RESULTS AND DISCUSSION

The spectral-element scheme has been shown to be efficient and accurate (11). Here, a sample of the results is presented, demonstrating the versatility of the types of numerical experiments that may be undertaken, and the potential usefulness in developing a fundamental understanding for a range of practical problems.

Figure 2 shows a typical predicted non-dimensionalised time sequence, showing the boundary deformation, translation and velocity magnitude of a Newtonian droplet. For this benchmark sequence, Re = 1000, We = 15, η_d/η_g = 16, ρ_d/ρ_g = 550.

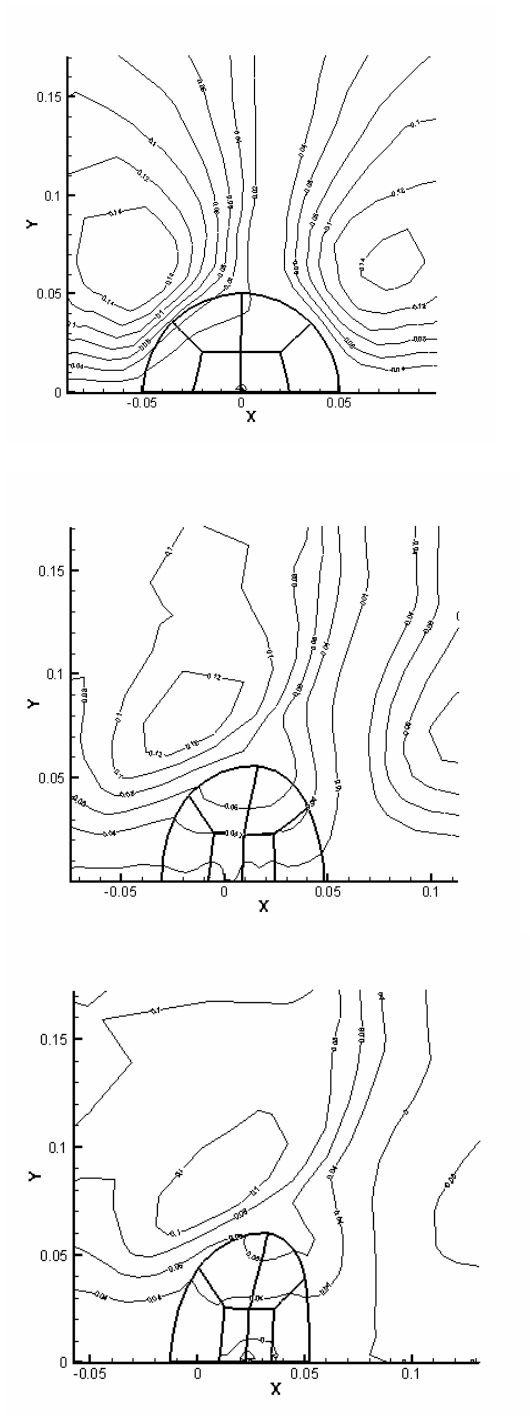

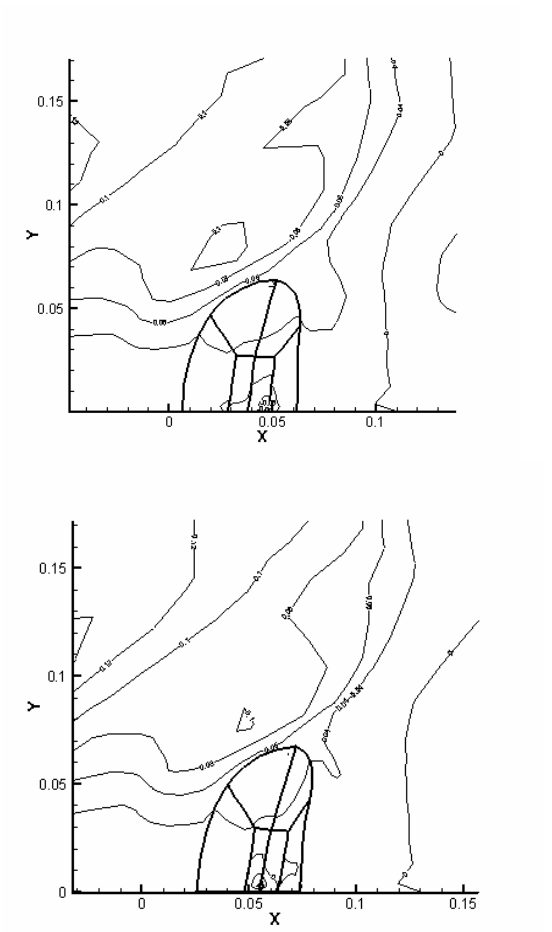

Figure 2. Predicted Droplet Deformation, Translation and Velocity Magnitude Contours - Benchmark Newtonian Problem. T = 0.03, 0.15, 0.21, 0.27, 0.33

First, note that the droplet starts accelerating with the flow due to the drag force, and also relatively smoothly starts to deform, reducing its 'waist', whilst elongating in the vertical direction.

Though not shown in these selective global images, the extremities of the deformed droplet in fact reverses its direction of movement relative to the nominal 'centre' of the moving, deforming droplet, i.e. first moves against the flow, before sweeping back to align itself with the flow for the remainder of the time interval.

This may be observed more clearly in Figure 3, where three cases for differing Reynolds and Weber number are presented. Here it is noted that for low Weber number (We = 1), the extremities of the droplet first move away from the centre in the upstream direction, before relaxing and seemingly asymptotically approaching a constant deformation in the upstream direction (i.e. $x_k < 0$). This is associated with the increased influence of surface tension at the lower Weber number. By contrast, for higher Weber number (We = 15), the droplet extremities again first move in the upstream direction, before reversing and continuing to deform in the downstream direction with time, due to less resistance to change of shape offered by surface tension forces.

For high Weber number and lower Reynolds number, the droplet oscillates during the dominant period of elongation in the downstream direction. The oscillations appear to dampen out for higher Reynolds number as the

deformation process becomes more stable as the influence of inertia dominates over viscous forces.

It is of interest to consider the influence of large changes in fluid viscosity, with the contemporary interest of utilisation of vegetable oil as a fuel for power generation applications. Figure 4 shows the difference in deformation occurring at roughly the same instant in time for the same benchmark problem. All parameters apart from viscosity ratio – which is increased by an order of magnitude – are kept constant. In this case it is clearly visible that minimal boundary deformation has taken place compared with the corresponding time instant for the benchmark case - the final image in Figure 2.

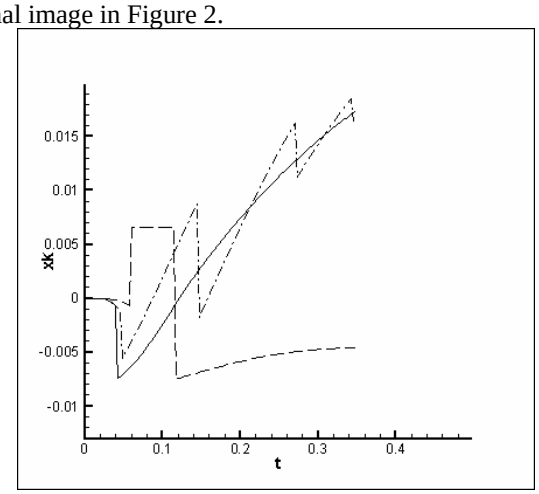

Figure 3. Evolution of the Lateral Displacement of the position of Maximum Axial Deformation relative to the Droplet Origin for 3 Cases : η_d/η_g = 16, ρ_d/ρ_g = 550, (i) Full Line – We = 15, Re = 1000, (ii) Dash Line – We = 1, Re = 1000, (iii) Dot-Dash line – We = 15, Re = 100

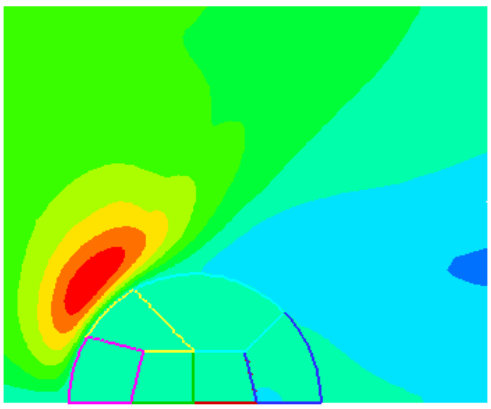

Figure 4. Droplet Deformation and Velocity Magnitude Contours of a Liquid Droplet in a Flow at 10x the Viscosity Ratio compared with Benchmark Case, all other parameters constant

Finally, consideration is given to the prediction of deformation of the non-Newtonian fluid. In terms of practical relevance, the Cross model fluid parameters have been chosen to represent a nominal sample of blood (12), though it is appreciated that blood requires more sophisticated visco-elastic modelling for more realistic predictions in complex flows (13).

The benchmark case is again considered, but with the four additional parameters required for the Cross model taken from (12) for blood to be :η_0 = 125 mPa.s, η_∞ = 5 mPa.s, K = 52.5 s and m = 0.715. The degree of shear thinning is represented by the value of m, where m approaching zero tends towards the Newtonian fluid, whilst m approaching 1 indicates the most shear-thinning fluids. Hence, in this model blood is considered to show significant shear thinning characteristics. Atomisation of blood has been known to be influential in homicide legal cases, where differences in blood spray at the scene require differentiating in terms of the atomisation source (e.g. spray due to impact, involuntary oral spray release due releasing blood collecting in bodily air passages, etc..).

Significant variation in deformation topology from the Newtonian case is visible in Figure 5, as the droplet now extends laterally – in the direction of flow - rather than in orthogonal to the flow. These findings require considerable further investigation, which is ongoing.

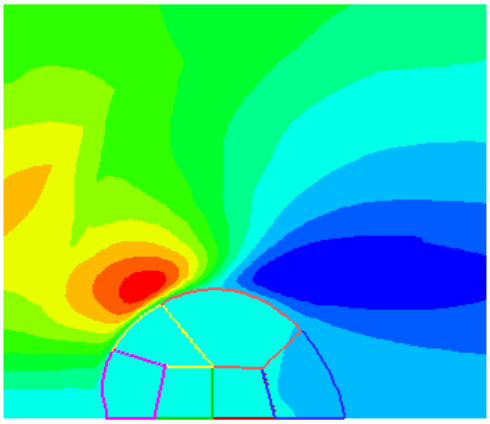

Figure 5. Droplet Deformation and Contours of Velocity Magnitude for a Blood Droplet represented by the Shear-thining Model of Cross (10)

6 CONCLUSIONS

(1) A new DNS of droplet deformation based on Spectral Element spatial discretisation coupled with an arbitrary Lagrangian Eulerian (ALE) treatment of the free boundary, has facilitated study of a Newtonian and non-Newtonian fluid droplet translating and deforming in a second Newtonian fluid medium.

(2) The governing Newtonian two-fluid system of equations has been neatly non-dimensionalised to express the problem in terms of four non-dimensionalised variables, each of practical relevance, and a 4-parameter non-Newtonian viscosity model has been introduced to further extend the range of fluids for which the model is applicable. Hence, it is possible to undertake parametric numerical experiments for each of the variables independently.

(3) Characteristic geometrical features of the deforming droplet vary with Weber number, whilst Reynolds number seems to influence the stability of the deformation, dampening out oscillatory behaviour.
(4) An increase in viscosity ratio minimises droplet deformation, whilst introducing the non-Newtonian model is shown to introduce unusual deformation topologies such as extension in the direction of flow, which require further studies and analyses.

7 NOMENCLATURE

$\mathbf{u}_i$, p_i – velocity field, pressure, for fluid i
Re, We – Reynolds number, Weber number
$\mathbf{T}i$, $\boldsymbol{\sigma}_i$ – extra, Cauchy stress tensor, for fluid i
$\mathbf{d}_i$ – rate of strain tensor, for fluid i
κ - local radius of curvature of fluid interface
R_1, R_2 - the principal radii of curvature at interface
η,η_0,η_∞ - viscosity function, zero shear-rate viscosity, high shear-rate viscosity asymtote
K, m - parameters of the Cross model
w - reference frame velocity
$A_{i,j},B,C_i,D_i,F_i$ – matrices in weak formulation of governing equations
$\mathbf{X}_i$ - nodal co-ordinates of mesh
D - parent element in tranfinite mapping operation
u_N, p_N - spectral expansion in terms of basis functions
ϕ_j, ψ_k - global basis functions for spectral expansion
u_j, p_k - components of spectral expansion
A_N,B_N,C_N - matrices representing the governing equations
t - non-dimensionalised time
x_k - distance between 'centre' of moving droplet and horizontal position of maximum axial deformation

8 REFERENCES

1. Pilch M. and Erdman C.A., *Use of Breakup Time Data and Velocity History Data to Predict the Maximum Size of Stable Fragments for Acceleration-Induced Breakup of a Liquid Drop*, Int. J. Multiphase Flow, 1987, **13**, No.6, p.741-757
2. Shraiber A.A., Podvysotsky A.M. and Dubrovsky V.V., *Deformation and Breakup of Drops by Aerodynamic Forces*, Atomisation and Sprays, 1996, **6**, p.667-692.
3. Comer, M.A., Bowen P.J., Sapsford S.M. and Kwon S.J., *A Parametric Sensitivity Study of GDI Spray Characteristics using a 3D Transient Model*, Int. J. Automotive Technology, 2005.
4. Hirt C.W., Amsden A.A. and Cook J.L., *An Arbitrary Lagrangian-Eulerian Computing Method for All Flow Speeds*, J.Comput. Phys., 1974, **14**, p.227-253.
5. Noh W.F., *A Time-Dependent Two-Space Dimensional Coupled Eulerian-Lagrangian Code*, In. Adler B., Fernback S. and Rotenberg M., editors, Methods in Computational Physics 3, Academic Press, New York, 1964.
6. Donea J., Giuliani S. and Halleux J.P., *An Arbitrary Lagrangian-Eulerian Finite Element Method for Transient Fluid-Structure Interactions*, Comput. Meth. Appl. Mech. Engrg, 1982, **33**, p.689-723.
7. Belytschko T., Kennedy J.M. and Schoeberie D.F. *Quasi-Eulerian Finite Element Formulation for Fluid Structure Interaction*, ASME J.Pressure Vessel Technol., 1980, **102**, p.62-69
8. Hellenbrock B.T. and Edwards C.F. , *A two-fluid Spectral Element Method with Application to Drops*, Proc. 8th ICLASS, Pasedena, CA, 2000
9. Deng Z-T, Jeng S-M, *Numerical Simulation of Droplet Deformation in Convective Flows*, AIAA Journal, 1992, **30**, No.5, p. 1290-1297.
10. Cross M.M, J. Colloid Sci., 1965, **20**, p.417-.
11. Bowen P.J., Phillips T.N. and Zheng Y. *The Prediction of Droplet Deformation using a Spectral ALE Method*, submitted to J. Comput. Phys, 2006
12. Barnes H.A., Hutton J.F. and Walters K. An Introduction to Rheology, Elsevier, Amsterdam, 1989.
13. R. G. Owens, *A new microstructure-based constitutive model for human blood*. J. Non-Newtonian Fluid Mech. (2006), accepted for publication.